European Journal of Pharmaceutical Sciences 151 (2020) 105395

Contents lists available at ScienceDirect

European Journal of Pharmaceutical Sciences

journal homepage: www.elsevier.com/locate/ejps

Fluorescent probes for the dual investigation of MRP2 and OATP1B1 function and drug interactions

Virág Székely[a,b], Izabel Patik[a], Orsolya Ungvári[a], Ágnes Telbisz[c], Gergely Szakács[a,d], Éva Bakos[a], Csilla Özvegy-Laczka[a,*]

[a] Membrane protein research group, Institute of Enzymology, Research Centre for Natural Sciences, H-1117 Budapest, Hungary
[b] Doctoral School of Molecular Medicine, Semmelweis University, H-1085 Budapest, Hungary
[c] Biomembrane research group, Institute of Enzymology, RCNS, H-1117 Budapest, Hungary
[d] Institute of Cancer Research, Medical University Vienna, Borschkegasse 8a, 1090 Wien, Austria

ARTICLE INFO

Keywords:
OATP
MRP2
ABCG2
Fluorescent dye
Transcellular assay
Drug interaction

ABSTRACT

Detoxification in hepatocytes is a strictly controlled process, in which the governed action of membrane transporters involved in the uptake and efflux of potentially dangerous molecules has a crucial role. Major transporters of hepatic clearance belong to the ABC (ATP Binding Cassette) and Solute Carrier (SLC) protein families. Organic anion-transporting polypeptide OATP1B1 (encoded by the SLCO1B1 gene) is exclusively expressed in the sinusoidal membrane of hepatocytes, where it mediates the cellular uptake of bile acids, bilirubin, and also that of various drugs. The removal of toxic molecules from hepatocytes to the bile is accomplished by several ABC transporters, including P-glycoprotein (ABCB1), MRP2 (ABCC2) and BCRP (ABCG2). Owing to their pharmacological relevance, monitoring drug interaction with OATP1B1/3 and ABC proteins is recommended. Our aim was to assess the interaction of recently identified fluorescent OATP substrates (various dyes used in cell viability assays, pyranine, Cascade Blue hydrazide (CB) and sulforhodamine 101 (SR101)) (Bakos et al., 2019; Patik et al., 2018) with MRP2 and ABCG2 in order to find fluorescent probes for the simultaneous characterization of both uptake and efflux processes. Transport by MRP2 and ABCG2 was investigated in inside-out membrane vesicles (IOVs) allowing a fast screen of the transport of membrane impermeable substrates by efflux transporters. Next, transcellular transport of shared OATP and ABC transporter substrate dyes was evaluated in MDCKII cells co-expressing OATP1B1 and MRP2 or ABCG2. Our results indicate that pyranine is a general substrate of OATP1B1, OATP1B3 and OATP2B1, and we find that the dye Live/Dead Violet and CB are good tools to investigate ABCG2 function in IOVs. Besides their suitability for MRP2 functional tests in the IOV setup, pyranine, CB and SR101 are the first dual probes that can be used to simultaneously measure OATP1B1 and MRP2 function in polarized cells by a fluorescent method.

1. Introduction

The liver has a central role in the defense of the body against harmful compounds. Membrane transporters expressed in hepatocytes are key players in the elimination of potentially toxic compounds of endogenous or exogenous origin (Jetter and Kullak-Ublick, 2019). Na^+-and ATP-independent uptake of bile acids, bilirubin, steroid hormones and several drugs from the blood into the liver is mediated by members of the Organic anion-transporting polypeptides family, OATP1B1, OATP1B3 and OATP2B1 (Dawson et al., 2009; Hagenbuch and Stieger, 2013). Conversely, following metabolism by hepatic enzymes, modified compounds are effluxed from hepatocytes into the bile or back to the blood stream by the action of ABC (ATP Binding Cassette) transporters including P-glycoprotein (ABCB1), MRPs (ABCC family) and BCRP (ABCG2) (Kock and Brouwer, 2012). Coordinated action of hepatic OATPs and ABCs ensures efficient hepatobiliary elimination of their shared substrates.

OATP1B1, encoded by the SLCO1B1 gene is exclusively expressed in the sinusoidal membrane of hepatocytes (Konig et al., 2000), and is the most abundant OATP of the human liver (Badee et al., 2015; Kimoto et al., 2012; Prasad et al., 2014). OATP1B1 is an organic anion exchanger that mediates the cellular uptake of bile acids, bilirubin,

Abbreviations: CaAM, calcein acetoxy-methyl ester; CB, Cascade Blue hydrazide; DDI, drug-drug interaction; FMTX, fluorescein-methotrexate; IOV, inside-out membrane vesicles; LDV, Live/Dead Violet; LDG, Live/Dead Green; LY, Lucifer Yellow; SR101, sulforhodamine 101

* Corresponding author.
E-mail address: laczka.csilla@ttk.mta.hu (C. Özvegy-Laczka).

https://doi.org/10.1016/j.ejps.2020.105395
Received 6 December 2019; Received in revised form 27 April 2020; Accepted 25 May 2020
Available online 29 May 2020

thyroid and sex hormones, and also that of numerous clinically applied drugs (Roth et al., 2012). OATP1B1 is a site of drug-drug interactions (DDIs), inhibition of its function results e.g. in statin-induced myopathy (Link et al., 2008; Shitara, 2011; Shitara et al., 2003).

MRP2 (ABCC2) is expressed in the canalicular membrane of hepatocytes (Jedlitschky et al., 2006) where it mediates the active efflux of conjugated and unconjugated organic anions (e.g. bilirubin and steroid conjugates), and also the co-transport of uncharged molecules with glutathione into the bile (Konig et al., 1999). Mutations in OATP1B (SLCO1B) or MRP2 (ABCC2) genes both lead to increased serum bilirubin levels respectively termed as Rotor or Dubin Johnson syndrome, indicating that bilirubin elimination through the liver requires the function of OATP1B1/3 and MRP2 (van de Steeg et al., 2012) (Konig et al., 1999). Besides its endogenous substrates, MRP2 also recognizes various drugs (Jedlitschky et al., 2006). Hence, by mediating the extrusion of metabolites from hepatocytes into the bile, MRP2 plays a key role in the terminal phase of detoxification (Zhou et al., 2008).

Similarly to MRP2, BCRP (ABCG2) is also expressed in the canalicular membrane of hepatocytes (Horsey et al., 2016; Maliepaard et al., 2001) and is involved in the hepatobiliary excretion of various organic compounds (Hirano et al., 2005; Lee et al., 2015; Patel et al., 2016). ABCG2 is a genuine multidrug transporter, recognizing a plethora of chemically diverse molecules that includes chemotherapeutics, statins, anti-HIV drugs and antibiotics (Doyle et al., 1998; Horsey et al., 2016). Given its wide substrate recognition pattern, ABCG2 is also a site of DDI (Lee et al., 2015; Mao and Unadkat, 2015). ABCG2 transports several endogenous substrates such as urate, haem and estrogen conjugates (estradiol-glucuronide and estrone sulfate) (Heyes et al., 2018). The most common ABCG2 polymorphism c.421C>A (p.141Q>K, rs2231142) is associated with gout, due to the mislocalization of the protein (Matsuo et al., 2009; Woodward et al., 2009). Significantly, SNPs in ABCG2 have been correlated with the altered pharmacokinetics of statins and sulfasalazin (Giacomini and Huang, 2013; Heyes et al., 2018). Thus, MRP2, ABCG2 and OATP1B1 have overlapping substrate specificities. They are important determinants of hepatobiliary excretion of various drugs, including chemotherapeutics, statins and anti-HIV agents (Giacomini et al., 2010; Hooijberg et al., 1999; Kitamura et al., 2008; Liu et al., 2010; Roth et al., 2012). Therefore co-administration of their substrates can lead to serious side effects, underlying the relevance of these transporters as sites of DDIs. Hence, according to the recommendations of the US Food and Drug Administration (FDA) and the European Medicines Agency (EMA), interactions with OATP1B1/3 and ABCG2 (and also potentially with MRP2) should be assayed during drug development. FDA and EMA regulations require the use of sensitive and reliable functional assays for the evaluation of transporter drug interactions (Giacomini et al., 2013).

Radioactively labeled substrates, such as bromosulphophtalein, leukotriene C_4, dehydroepiandrosterone sulfate (DHEAS), estrone-3-sulfate (E1S) or estradiol-17β-D-glucuronide (E217G) have been repeatedly used for the characterization of OATP and ABC transporter function and for the study of DDIs (Cui et al., 2001; Hirouchi et al., 2009; Liu et al., 2006; Matsushima et al., 2005). In general, a limitation of the radioligand transport assays is the cost associated with the radiolabeling of the substrates. Fluorescence assays offer a cost effective alternative, and it was shown that fluorescent probe substrates provide an effective and sensitive means to investigate transporter function and drug-transporter interactions (Szakacs et al., 2008). Since the discovery of Calcein-AM to probe P-glycoprotein and MRP function more than two decades ago (Hollo et al., 1994), the list of fluorescent MRP2 substrates has expanded (Cantz et al., 2000; Notenboom et al.,2005; Prevoo et al., 2011; Siissalo et al., 2009). Similarly, fluorescent dye substrates of ABCG2 (Hoechst, DyeCycle Violet) have long been used to investigate its function or drug interactions (Mathew et al., 2009; Ozvegy et al., 2002). Whereas the study of the efflux function of ABC transporters requires the use of dyes that can accumulate in the cells (high passive uptake) (Szakacs et al., 2008), ideal test substrates measuring OATP function are cell impermeable (Bednarczyk, 2010; Gui et al., 2010; Kovacsics et al., 2017; Patik et al., 2018; Yamaguchi et al., 2006).

To date, fluorescent probes allowing the simultaneous investigation of OATP1B1 and the hepatic ABC transporters have not been identified. The goal of the current work was to analyze the interaction of fluorescent OATP1B1 substrates with MRP2 and ABCG2 in order to find dual OATP ABC transporter probes. Our earlier work has identified Zombie Violet (ZV), Live/Dead Violet (LDV), Live/Dead Green (LDG), Cascade Blue hydrazide (CB), Alexa Fluor 405 (AF405) (Patik et al., 2018), and recently SR101 (sulforhodamine 101) (Bakos et al., 2019) as novel fluorescent substrates of OATP1Bs. We have also shown that CB and AF405 can be applied as probes in OATP1B1/3 or OATP2B1 drug interaction tests (Patik et al., 2018). Since these OATP probes are cell-impermeant, their transport by ABCG2 or MRP2 cannot be directly investigated in cellular assays. However, transporter-mediated accumulation of the same dyes can be measured in inside-out vesicles (IOVs). Because of the reverse orientation of the membrane lipid bilayer and the efflux transporters, ATP-dependent uptake of a substrate into IOVs corresponds to cellular efflux, allowing the measurement of the transport of cell impermeable dyes by ABC efflux transporters. Using this experimental setup, we show that several cell-impermeable fluorescent substrates are indeed transported by MRP2 and ABCG2. Theoretically, cellular efflux may be measured if the accumulation of the cell impermeable dyes was facilitated by uptake transporters. Using double-transfected, polarized MDCKII cells overexpressing OATP1B1 and MRP2 or ABCG2, we identify dual OATP1B1 and MRP2 fluorescent probes, setting the stage for a fluorescence-based assay development measuring vectorial transport mediated by these transporters.

2. Materials and methods

2.1. Materials

Zombie Violet was purchased from BioLegend® (San Diego, CA, US). LIVE/DEAD® Fixable Cell Stain Dyes (Violet and Green), fluorescein-methotrexate and Cascade Blue hydrazide were purchased from Thermo Fisher Scientific (Waltham, MA, US). All other materials, if not indicated otherwise, were from Sigma Aldrich, Merck (Budapest, HU).

2.2. Generation of cell lines and cell culturing

A431 cells expressing OATPs 1B1, 1B3 or 2B1 and their mock transfected counterparts were generated previously as described in Patik et al. (2018). The MDCKII-MRP2 cell line was generated previously (Bakos et al., 2000). In order to generate MDCKII cells expressing ABCG2, MDCKII parental cells were transfected with 1 μg plasmid DNA (pSB-CMV-ABCG2, allowing transposon mediated genomic insertion of ABCG2 cDNA (Saranko et al., 2013)) and 100 ng plasmid containing the 100x Sleeping Beauty transposase using Lipofectamine 2000® reagent (Thermo Fisher Scientific) according to the recommendation of the manufacturer. After 48 hours the transfection medium was removed and the cells were selected in puromycin (1 μg/ml) for two weeks. Transfected cells were sorted based on labeling by the anti-ABCG2 monoclonal antibody 5D3 (Bioscience), which binds to a surface epitope (Ozvegy et al., 2002). Cells showing 5D3 positivity were sorted using a BD FACSAria III Cell Sorter (BD Biosciences, San Jose, CA, US).

OATP1B1 expression in MDCKII, MDCKII-MRP2 or MDCKII-ABCG2 cells was achieved by recombinant lentiviruses as described earlier (Patik et al., 2018). Briefly, MDCKII parental, MDCKII-MRP2 and MDCKII-ABCG2 cells were transfected with the pRRL-CMV-OATP1B1-MCS-IRES-ΔCD4 vector. In order to generate mock transfected control cells for transport experiments, MDCKII cells were transfected with the pRRL-EF1-ΔCD4 vector. Transduced cells were sorted based on their CD4 positivity using a BD FACSAria III Cell Sorter (BD Biosciences, San

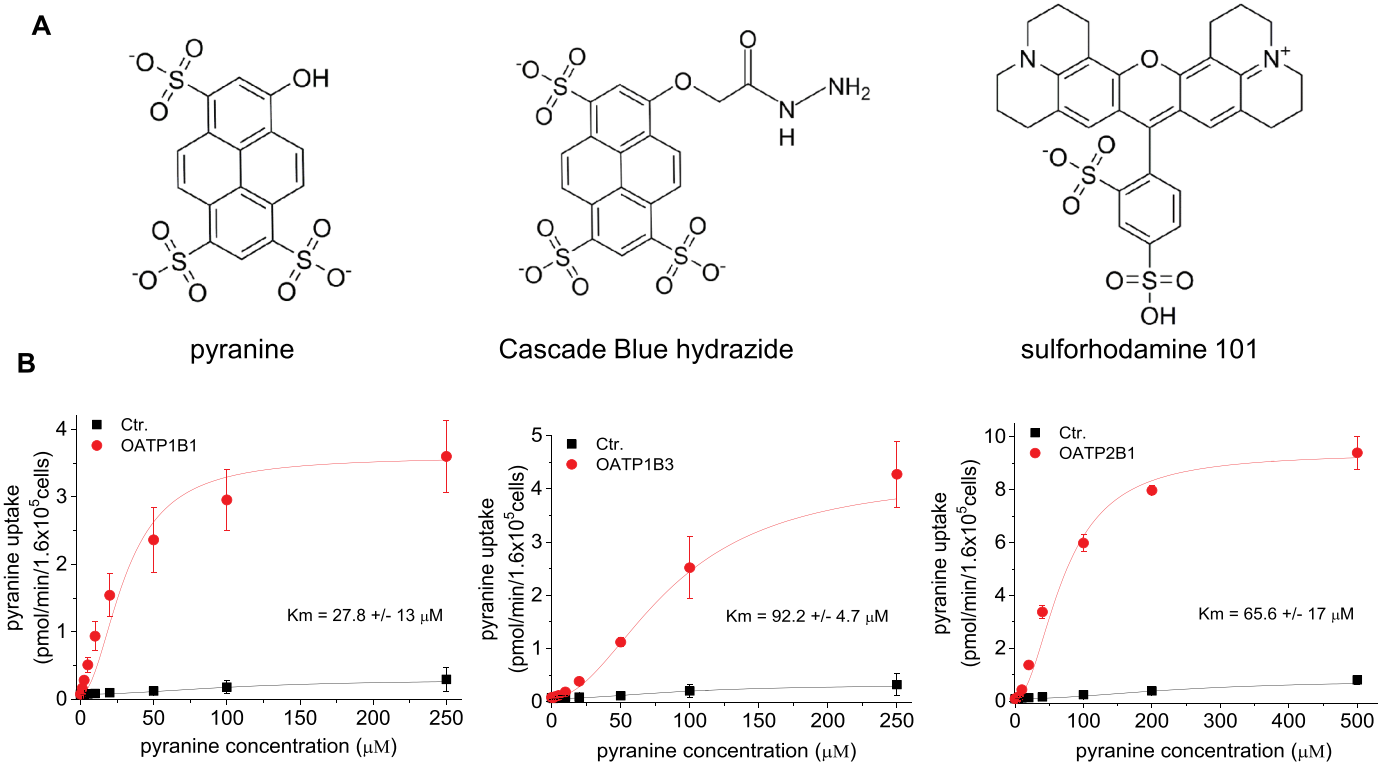

Fig. 1. A) Structure of the dyes tested in the current study. B) Pyranine is a novel substrate of OATP1B1, OATP1B3 and OATP2B1. Concentration dependent uptake of pyranine was measured in A431 cells overexpressing OATP1B1, OATP1B3 or OATP2B1, or mock transfected controls (Ctr.) seeded onto 96-well plates at 37°C in the linear phase of transport, at 10 (OATP1B1) or 15 (OATP1B3 and OATP2B1) minutes at pH 5.5. Fluorescence was determined using an Enspire plate reader (Ex/Em: 403/517 nm). Transport kinetics was determined by subtracting fluorescence measured in mock transfected cells. Average +/- SD values of at least 3 independent measurements are shown.

Jose, CA, US). OATP1B1 overexpressing cells were sorted based on their increased Live/Dead Green uptake, as described earlier (Patik et al., 2018).

A431 and MDCKII cells were grown in DMEM (Gibco, Thermo Fisher Scientific (Waltham, MA, US)) completed with 10 % fetal bovine serum, 2 mM L-glutamine, 100 U/ml penicillin, and 100 μg/ml streptomycin at 37°C, 5% CO_2, under sterile conditions.

2.3. Western blot

MDCKII cell lysates were separated on 7.5% Laemmli SDS-PAGE gels and transferred onto PVDF membranes. Immunoblotting was performed as described (Sarkadi et al., 1992). Membranes were incubated overnight with anti-OATP1B1, anti-MRP2 (M_2-I-4 / M_2-III-6 monoclonal antibody) (Bakos et al., 2000) or anti-ABCG2 (BXP-21, Maliepaard et al., 2001) antibodies or anti-β-actin antibody (A1978, Sigma). The antibody used for the detection of OATP1B1 was a kind gift from Dr. Bruno Stieger (Department of Clinical Pharmacology and Toxicology, University Hospital, 8091 Zurich, Switzerland) (Kullak-Ublick et al., 2001). Secondary antibodies were HRP-conjugated anti-rabbit (OATP1B1) or anti-mouse (MRP2, ABCG2, ß-actin) antibodies (Jackson ImmunoResearch, Suffolk, UK) in a dilution of 20,000x. Luminescence was detected using the Luminor Enhancer Solution kit by Thermo Scientific (Waltham, MA, US).

2.4. MRP2 and ABCG2 expression in insect cells and inside-out membrane vesicle preparation

Recombinant baculovirus containing the ABCC2/MRP2 cDNA (Bakos et al., 2000), ABCG2 cDNA (Ozvegy et al., 2002) or the cDNA of an unrelated protein (Patik et al., 2015) were used to achieve transient expression in *Sf9* insect cells. Culturing and infection of *Sf9* cells was performed as described earlier (Sarkadi et al., 1992). Virus-infected *Sf9* cells were harvested after 72 hours. Following washing with Tris-mannitol buffer (50 mM Tris, pH 7.0, with HCl, 300 mM mannitol and 0.5 mM phenylmethylsulfonyl fluoride), cells were lysed and homogenized in TMEP (50 mM Tris, pH 7.0, with HCl, 50 mM mannitol, 2 mM EGTA, 10 μg/ml leupeptin, 8 μg/ml aprotinin, 0.5 mM phenylmethylsulfonyl fluoride, and 2 mM dithiotreitol) using glass tissue grinder tubes. Undisrupted cells were removed by centrifugation for 10 min at 500 g. Finally, the supernatant containing the membranes was centrifuged for 1 h at 100 000 g, and the pellet was resuspended in TMEP (with freshly appended 0.5 mM phenylmethylsulfonyl fluoride) at concentration of 5-10 mg/ml. Membranes were stored at -80°C in aliquots. (Bakos et al., 2000; Sarkadi et al., 1992). In the case of ABCG2 cholesterol enriched membranes IOVs were prepared in order to achieve maximal ABCG2 activity (Telbisz et al., 2007). Cholesterol loading was performed by incubation of the membranes (containing ABCG2 or their controls) with TMEP containing 2 mM Cholesterol-RAMEB (Cyclolab, Hungary) on ice for 30 minutes, prior to the final centrifugation step (Telbisz et al., 2007).

2.5. Transport measurements in inside-out vesicles

Membrane vesicles (50 μg/tube) were incubated in transport buffer (Bakos et al., 2000) with 4 mM MgATP or 4 mM MgAMP and with the fluorescent dyes 1 μM sulforhodamine 101 (SR101)/fluorescein-methotrexate (FMTX), 5 μM pyranine/Cascade Blue (CB), 10 μM Lucifer Yellow (LY) or 0.2 μl/tube ZV/LDV/LDG for 10 (ZV/LDV/LDG/FMTX/SR101/LY) / 20 (pyranine) / 30 (CB) minutes in 150 μl final volume at 37°C. These experimental conditions were evaluated by measuring time- and concentration dependent transport of the fluorescent dyes in preliminary experiments. For each compound, time and concentration values yielding the highest signal/noise ratio measured were chosen.

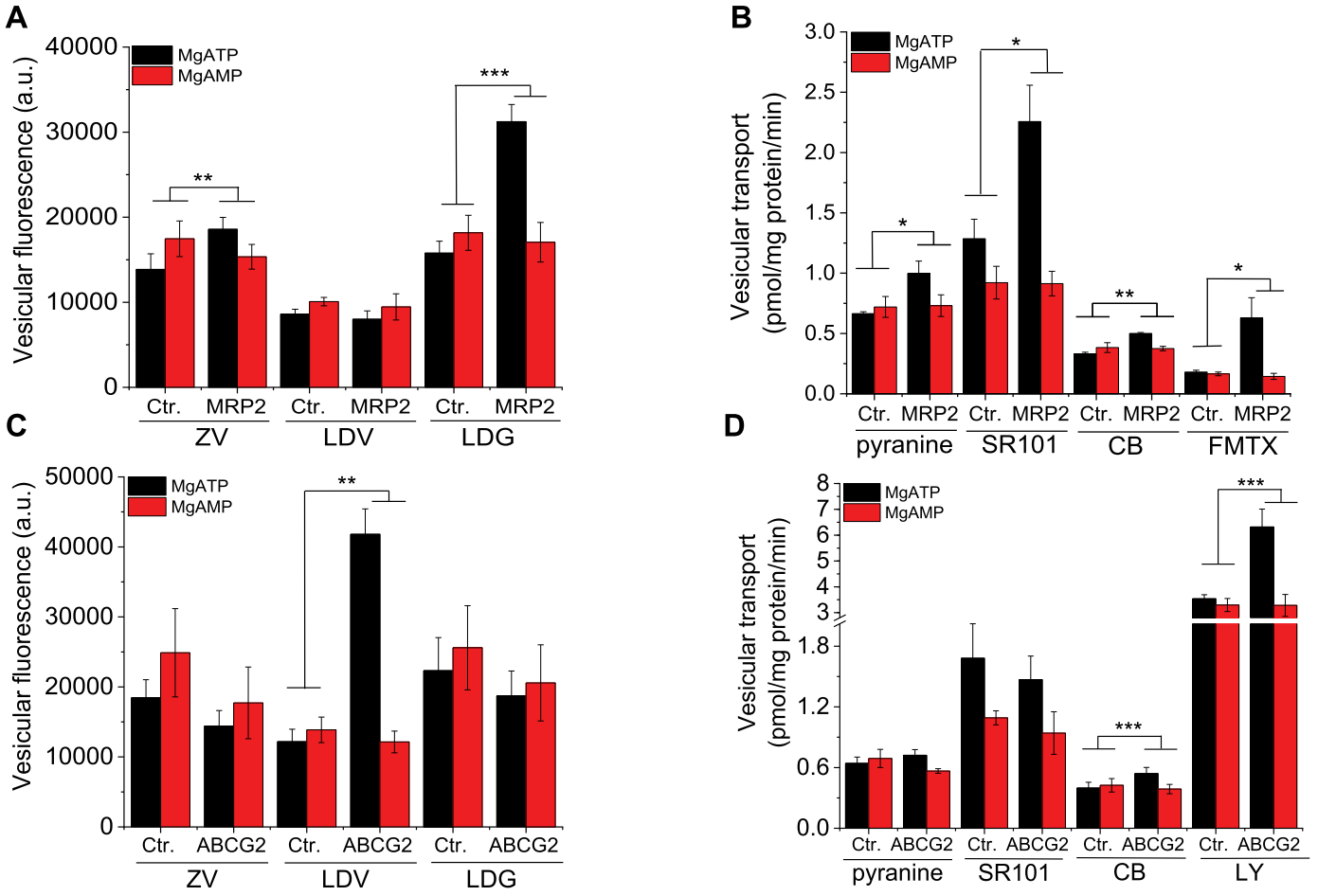

Fig. 2. Fluorescent dye transport measurements in inside-out membrane vesicles. Uptake of the fluorescent dyes, ZV, LDV and LDG (0.2 µl/sample), 5 µM CB, 5 µM pyranine, 1 µM SR101, 1 µM FMTX or 10 µM LY in MRP2- (panels A, B) or ABCG2- (panels C, D) containing or control membrane vesicles (50 µg) was measured for 30 minutes (CB), 20 minutes (pyranine) or 10 minutes (ZV, LDV, LDG, SR101, FMTX, LY) in the presence of 4 mM MgATP or 4 mM MgAMP at 37°C. Experiments were repeated 3-times. Average of at least 3 independent replicates +/- SD are shown. Statistical significance was calculated between ATP-dependent signals. Delta values generated by subtracting signals with MgAMP from that measured with MgATP were compared for statistical significance by Student's t-test, *: $p < 0.05$, **: $p < 0.01$, ***: $p < 0.001$.

When inhibition was investigated, the vesicles were pre-incubated with 1 µM Ko143, a known ABCG2 inhibitor (Allen et al., 2002) prior to the addition of the fluorescent dyes. Reaction was stopped by the addition of 550 µl ice cold transport buffer and by placing the samples on ice. Eppendorf tubes were centrifuged for 5 min at 22000 g. Supernatant was eliminated and the pellet was suspended in 200 µl RT (room temperature) 1 x Phosphate Buffered Saline (PBS). The suspensions were pipetted onto 96 well plates and fluorescence intensity was measured in an Enspire Fluorescent plate reader (Perkin Elmer) at the following wavelengths: 405/423 nm (ZV), 416/451 nm (LDV), 495/520 nm (LDG), 403/517 nm (pyranine), 400/419 nm (CB), 586/605 nm (SR101), 428/540 nm (LY), 497/516 nm (FMTX). Transport activity in the case of CB, pyranine, LY, SR101 and FMTX was determined based on a calibration curve.

2.6. Transport measurements in MDCKII cells by flow cytometry

MDCKII cells were collected following trypsinization (0.2% trypsin) in complete DMEM. After washing in 1 ml uptake buffer (125 mM NaCl, 4.8 mM KCl, 1.2 mM $CaCl_2$, 1.2 mM KH_2PO_4, 12 mM $MgSO_4$, 25 mM MES, and 5.6 mM glucose, with the pH adjusted to 5.5/7.4 using 1 M HEPES and 10 N NaOH for OATP/ABC function, respectively), 5×10^5 cells were incubated at 37°C for 10 min (calcein-AM (CaAM)) / 30 min (CB, DCV (DyeCycle Violet)) in 100 µl fluorescent dye (final concentrations: 0.5 µM CaAM, 1-1 µM CB or DCV) diluted in the appropriate buffer. CB/CaAM/DCV were used as substrates of OATP1B1/MRP2/ABCG2 for validating functionality. The reaction was stopped by the addition of 700 µl ice-cold 1 x PBS, and the samples were kept on ice until the flow cytometry analysis. Cellular fluorescence was determined of at least 20,000 living cells from each sample using an Attune Acoustic Focusing Cytometer (Applied Biosystems, Life Technologies, Carlsbad, CA, US).

2.7. OATP-mediated transport of pyranine using a microplate-based transport assay

Uptake of pyranine in A431 cells overexpressing OATPs 1B1, 1B3 or 2B1 was measured as described previously (Patik et al., 2018). Briefly, A431 cells (8×10^4/well) were seeded on 96-well plates in 200 µl DMEM one day prior to the transport measurement. Next day the medium was removed, and the cells were washed three times at room temperature with 1 x Phosphate Buffered Saline (PBS). The cells were pre-incubated with 50 µl uptake buffer (see above) at 37°C. The reaction was started by the addition of 50 µl uptake buffer containing increasing concentrations of pyranine. Cells were then incubated at 37°C for 10 minutes (OATP1B1) or 15 minutes (OATP1B3 and OATP2B1). The applied incubation time was evaluated during previous unpublished data. The reaction was stopped by removing the supernatant and washing the cells three times with ice-cold 1 x PBS. Wells were loaded with 200 µl ice-cold 1 x PBS and fluorescence was determined

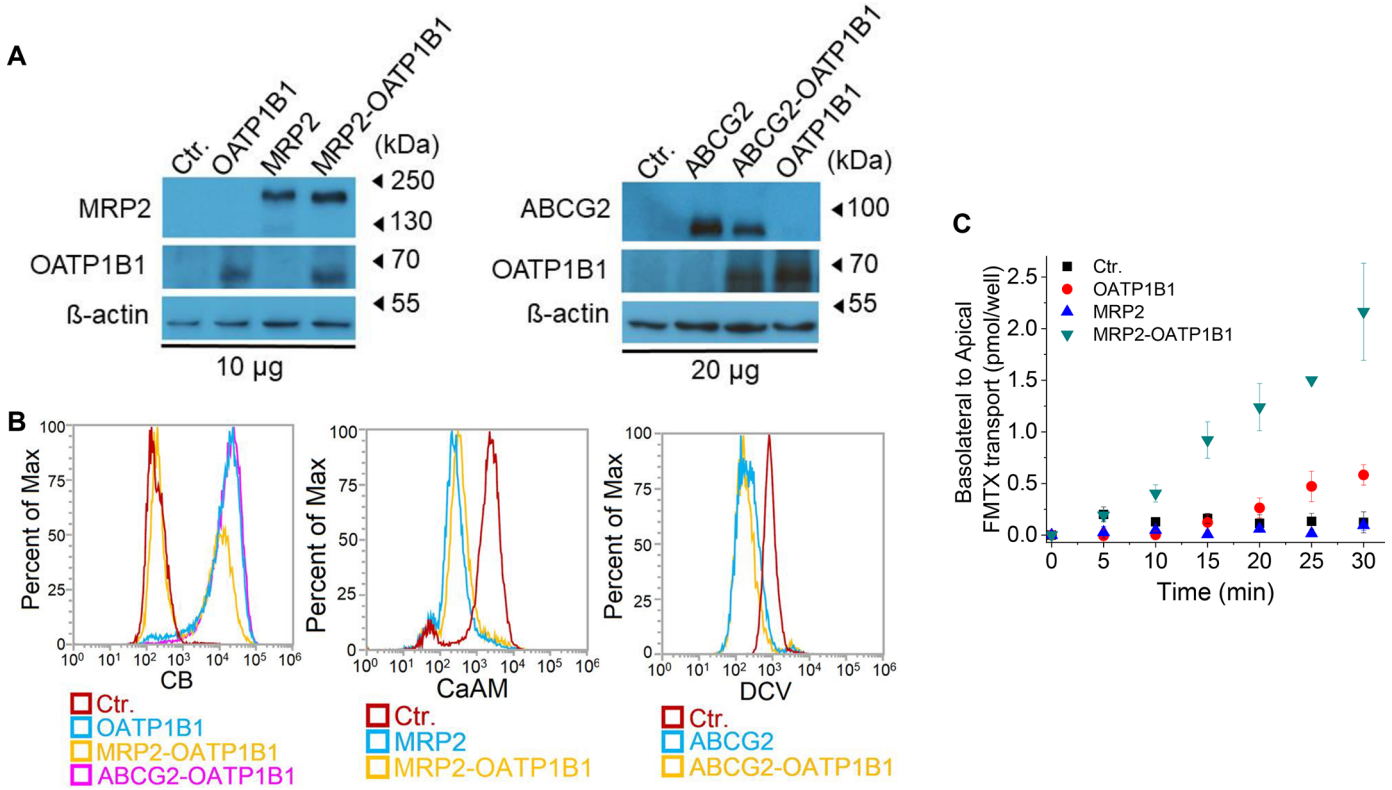

Fig. 3. Expression and function of OATP1B1, MRP2 or ABCG2 in the MDCKII cell lines. 3A: 10 or 20 µg of total cell lysates were analyzed for transporter expression by Western blot. Signals of OATP1B1/MRP2/ABCG2/ß-actin were visualized by the antibodies raised against these proteins. Transporter expression is equally present for OATP1B1/MRP2/ABCG2 among the appropriate cell lines. ß-actin signals verified the equal amount of proteins in the samples tested. Experiments were repeated at least 3-times. The result of one representative experiment is shown. 3B: Transporter function of OATP1B1, MRP2 or ABCG2 in MDCKII cell lines. Functionality of the transporters OATP1B1, MRP2 or ABCG2 was determined based on the transport of CB, CaAM or DCV substrates, respectively. 5×10^5 MDCKII cells were incubated at 37°C for 10 min (CaAM)/30 min (CB, DCV) in 100 µl fluorescent dye (final concentrations: 0.5 µM CaAM , 1-1 µM CB or DCV) diluted in the appropriate buffer (pH 5.5/7.4 for OATP/ABC function). Cellular fluorescence was determined of at least 20,000 living cells from each sample using an Attune Acoustic Focusing Cytometer (Applied Biosystems, Life Technologies, Carlsbad, CA, US). Transport measurements were repeated at least 3-times. One representative experiment is shown. 3C: Transcellular transport of fluorescein-methotrexate: Basolateral to apical transcellular transport of FMTX (1µM) in MDCKII-OATP1B1, MDCKII-MRP2, MDCKII-MRP2-OATP1B1 or control (Ctr., mock transfected) cells grown on transwell inserts for 4 days prior to the experiment was followed for 30 minutes at 37°C. Average of 3 independent measurements +/- SD are shown.

using an Enspire plate reader Ex/Em: 403/517 nm. OATP-dependent transport was determined by extracting fluorescence measured in mock transfected cells. Transport activity was calculated based on a calibration curve. Experiments were repeated in 3 biological replicates.

2.8. Transcellular transport measurements

For transcellular transport experiments, OATP1B1 and/or MRP2 or ABCG2 overexpressing MDCKII cells (9×10^4 cells/insert) were grown on Tissue culture plate inserts (6.5 mm diameter, 0.4 µM pore size, VWR Ltd., Hungary) for four days. The cells were seeded in 300 µl complete DMEM onto the insert membranes and 1 ml media was added to the wells around the inserts in 24 well plates. The transport measurement was started by the removal of the medium from the transwell inserts and by washing the cells two times with 300 µl pH 7.4 uptake buffer (see above). The wells were washed three times with 1 ml pH 5.5 uptake buffer (see above). After washing, 300 µl pH 7.4 buffer was pipetted into the inserts containing the cells and 1 ml pH 5.5 buffer into the wells and a 10 min pre-incubation period at 37°C was applied. The reaction was started by the addition of 1 ml uptake buffer pH 5.5 (ensuring higher OATP1B1 transport (Patik et al., 2018)) containing pyranine, CB, SR101, or FMTX (final concentrations 5-5 µM and 1-1 µM respectively) to the wells, and the tissue culture plates were further incubated at 37°C. When inhibitors were tested, 10 µM cyclosporin A (CsA) or 40 µM benzbromarone was added to the lower or upper compartment, respectively. To determine transport, 30 µl samples from the upper compartment were collected every 5 minutes and pipetted into 70 µl 1 x PBS for fluorescence measurements. In the case of MDCKII-ABCG2-OATP1B1 cells, CB transport was determined at the following time points: 0, 15 and 30 minutes. The fluorescence intensity of the samples was determined using an Enspire plate reader (Perkin Elmer) at the following wavelengths: 403/517 nm (pyranine), 400/419 nm (CB), 586/605 nm (SR101), or 497/516 nm (FMTX).

In order to evaluate the transport in the opposite direction (A-B), transport reaction was started from the apical side by adding the substrates at the same concentration as applied before but in 300 µl pH 7.4 buffer. Samples were collected from the wells (B side) to a 96 well plate, 100 µl at each time points until 25 minutes and fluorescence intensity was determined as described before.

For evaluating intracellular accumulation of pyranine, transport reaction in B-A direction was stopped after 30 minutes by removing the solutions from the wells and inserts and washing the cells three times with cold 1 x PBS on ice. Transwell inserts were then cut out and placed into 200 µl 1% Triton-PBS in Eppendorf tubes. Inserts were incubated at RT for 75 minutes, and then cell lysates were pipetted onto 96 well plates. Fluorescence intensity was determined using an Enspire plate reader as described above, Ex/Em: 403/517. In order to define the amount of the dyes in the samples, a calibration curve was generated by determining the fluorescence of increasing amounts of the given dye dissolved in 200 µl 1 x PBS. We found that fluoresce of the dyes

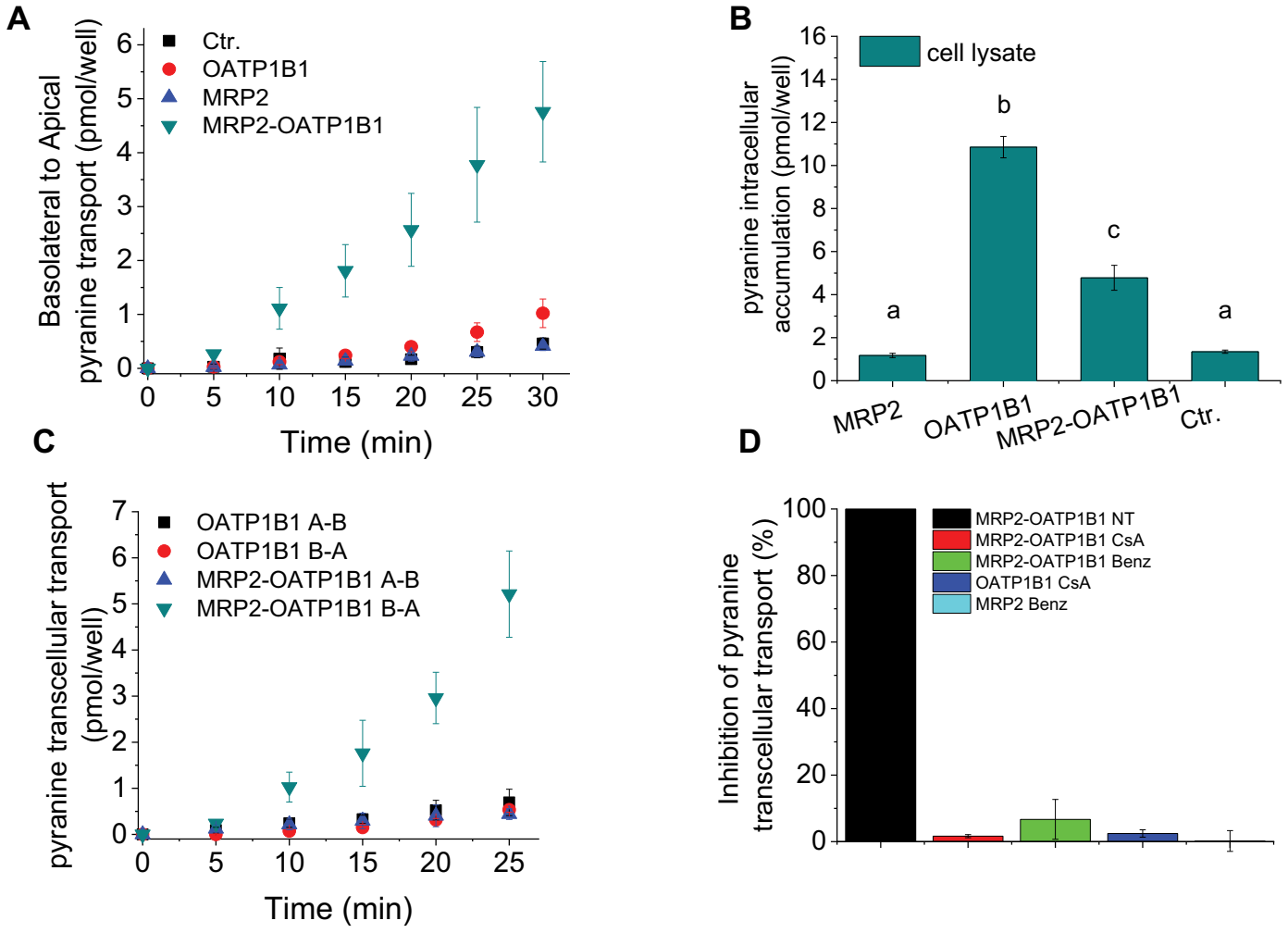

Fig. 4. Transcellular transport of pyranine. 4A: Basolateral to apical transport of pyranine (5 μM) in MDCKII-OATP1B1, MDCKII-MRP2, MDCKII-MRP2-OATP1B1 or control (Ctr., mock transfected) cells grown on transwell inserts for 4 days prior to the experiment was followed for 30 minutes at 37°C. Average of 5 independent measurements +/- SD are shown. 4B: Intracellular levels of pyranine were determined in MDCKII cells after 30 minutes of incubation with 5 μM pyranine administered from the basolateral side of the transwells. Average of 3 independent measurements +/- SD are shown. Statistical analysis for multi comparison was evaluated by Tukey-Kramer HSD (Honest Significant Differences) procedure, as a post-hoc test, after rejecting H_0 in One-Way ANOVA ($\alpha = 0{,}05$). Means +/- SD marked with the same letter ("a" for Ctr. and MRP2) were not significantly different ($p > 0.05$, Tukey-Kramer HSD test) from each other unlike "b" and "c" which mean significant difference. 4C: Lack of apical to basolateral transport of pyranine. Experiments were performed with pyranine (5 μM) added either to the apical or the basolateral compartment and samples were taken from the basolateral (A-B) or the apical compartment (B-A), respectively until 25 minutes. Average of 3 independent measurements +/- SD are shown. 4D: Inhibition of pyranine transcellular transport by cyclosporin A (CsA) or benzbromarone (Benz). Transcellular (B-A) transport of 5 μM pyranine can be inhibited by known OATP1B1 and MRP2 inhibitors, CsA and Benz. Vectorial transport was measured as described at Fig. 4A, except that 10 μM CsA or 40 μM benzbromarone was added to the basolateral or apical compartment, respectively prior to the addition of pyranine (5 μM). Fluorescence of pyranine was measured using an Enspire plate reader at Ex/Em 403/517 nm. Data obtained from 3 independent experiments +/- SD values are presented as a percent of transport measured in MDCKII-MRP2-OATP1B1 cells without any inhibitor (NT).

(pyranine, CB and SR101) diluted in PBS or accumulated in cells remained stable even after 90 minutes of incubation at room temperature (data not shown).

2.9. Data analysis and statistics

Kinetic parameters shown in Fig. 1B of dye uptake were analyzed by Hill1 fit using the OriginPro 8 software (GraphPad, La Jolla, CA, USA). Statistical significance was calculated by Student's t-test between ATP-dependent signals. Delta values were generated by subtraction of MgAMP or MgAMP + Ko signals from MgATP or MgATP + Ko signals, respectively. These delta values were compared for statistical significance by Student's t-test, *: $p < 0.05$, **: $p < 0.01$, ***: $p < 0.001$ (Figs. 2, 6).

Statistical analysis of the samples shown in Fig. 4B for multi comparison was evaluated by Tukey-Kramer HSD (Honest Significant Differences) procedure, as a post-hoc test, after rejecting H_0 in One-Way ANOVA ($\alpha = 0.05$). Samples marked with the same letter ("a" for MRP2 and Ctr.) were not significantly different from each other.

3. Results

3.1. Pyranine is a novel substrate of hepatic OATPs, 1B1, 1B3 and 2B1

To expand the scope of fluorescent OATP substrates, we evaluated the interaction of pyranine (HPTS, Solvent Green 7, trisodium 8-hydroxypyrene-1,3,6-trisulfonate), a pH indicator closely related to Cascade Blue hydrazide (CB) (Avnir and Barenholz, 2005; Clement and Gould, 1981; Gan et al., 1998) (Fig. 1) with OATP1B1, OATP1B3 and OATP2B1. Measurements were carried out using A431 cells overexpressing OATP1B1, OATP1B3 or OATP2B1. Whereas pyranine does not accumulate in control, mock transfected A431 cells (Fig. 1B), we

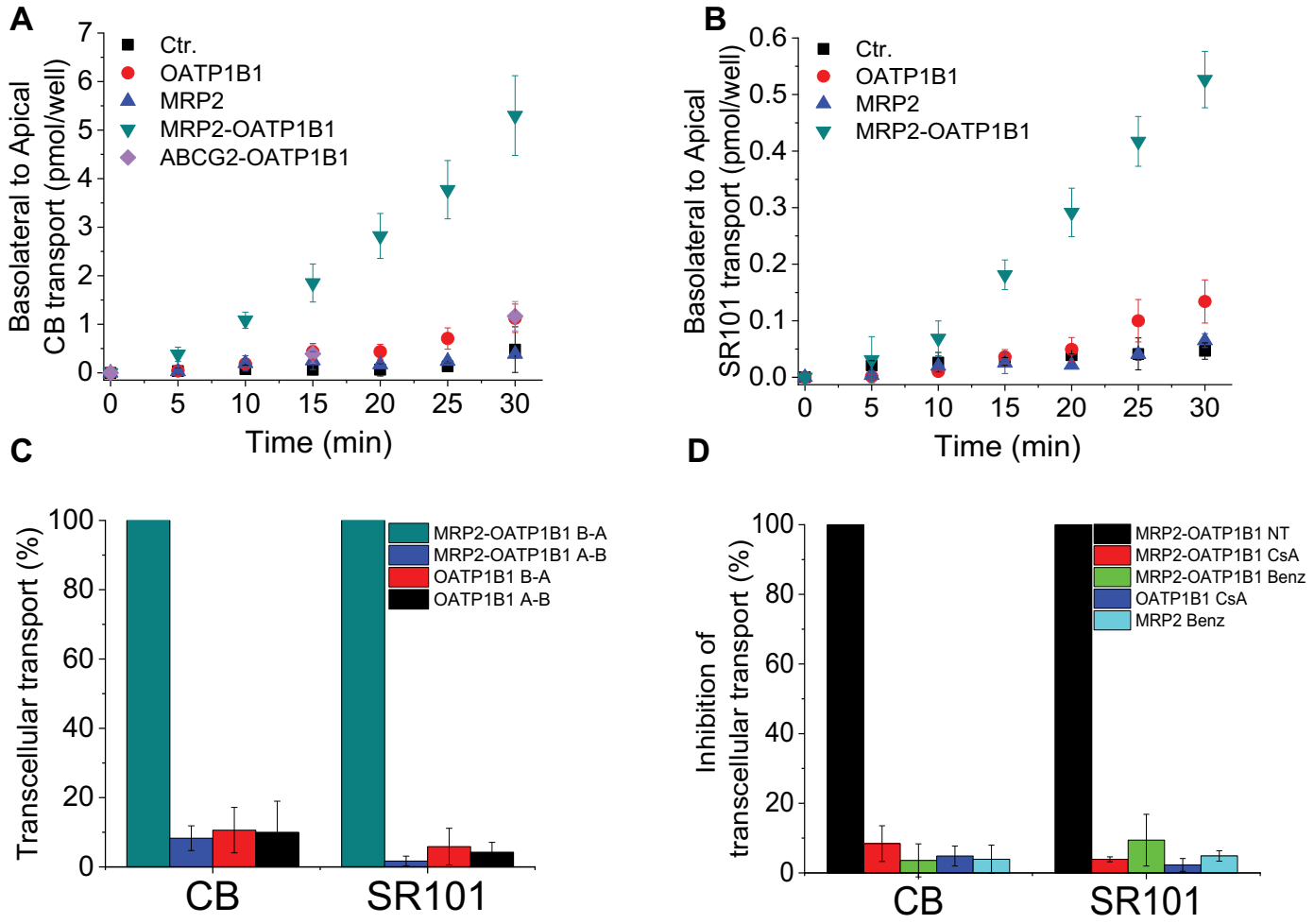

Fig. 5. Transcellular transport of Cascade Blue hydrazide or sulforhodamine 101. Basolateral to apical transport of CB (5 μM, panel A) or SR101 (1 μM, panel B) in MDCKII-OATP1B1, MDCKII-MRP2, MDCKII-MRP2-OATP1B1, MDCKII-ABCG2-OATP1B1 (panel A) or control (Ctr., mock transfected) cells grown on transwell inserts for 4 days prior to the measurement was followed for 30 minutes at 37°C. Average of 4 independent measurements +/- SD are shown for MDCKII-OATP1B1, MDCKII-MRP2, MDCKII-MRP2-OATP1B1 and Ctr. cells on panel A, and average of 3 independent measurements +/- SD are shown for MDCKII-ABCG2-OATP1B1 cells (panel A) and on panel B. 5C: Lack of apical to basolateral (A-B) transport of the fluorescent dyes. Experiment was performed on MDCKII cells grown on transwell inserts for 4 days prior to the measurement. CB (5 μM) or SR101 (1 μM) were added to the apical (A-B transport) or basolateral (B-A transport) compartment and after 25 minutes of incubation at 37°C samples were taken from the basolateral (A-B transport) or apical (B-A transport) compartment, and fluorescence was determined. Data are shown as a percent of B-A transport measured in MDCKII-MRP2-OATP1B1 cells. Average of 3 independent measurements +/- SD are shown. 5D: Inhibition of CB or SR101 transcellular transport. Transcellular (B-A) transport of 5 μM CB or 1 μM SR101 can be inhibited by known OATP1B1 and MRP2 inhibitors, cyclosporin A (CsA) and benzbromarone (Benz). Vectorial transport was measured as described at Fig. 4A, except that 10 μM CsA or 40 μM benzbromarone was added to the basolateral or apical compartment, respectively prior to the addition of the dyes 5 μM CB or 1 μM SR101. Data represent average +/- SD values of 3 independent experiments and are presented as a percent compared to the B-A transport measured in MDCKII-MRP2-OATP1B1 cells (NT).

found a typical OATP-mediated uptake in A431 cells expressing a hepatic OATP (Fig. 1B) revealing that pyranine is a common substrate of these uptake transporters.

3.2. Identification of novel common fluorescent substrates of OATP1B1, MRP2 and ABCG2

Hepatic OATPs and MRP2 or ABCG2 have an overlapping substrate recognition profile (Giacomini et al., 2010). To characterize the susceptibility of fluorescent OATP probes to MRP2 or ABCG2 mediated transport, we used inside-out membrane vesicles prepared from *Sf9* (*Spodoptera frugiperda*) cells overexpressing either MRP2 or ABCG2 (Fig. 2). IOVs allow the investigation of the transport of membrane impermeable substrates by efflux transporters that otherwise, in the lack of passive uptake, could not be investigated in cell-based assays with single transfectants. IOVs prepared from mock transfected *Sf9* cells, as well as transport in the presence of MgAMP served as negative controls for transport experiments. On the other hand, Lucifer Yellow (LY) and fluorescein-methotrexate (FMTX), documented substrates of ABCG2 or MRP2 (Deng et al., 2016; Notenboom et al., 2005; Prevoo et al., 2011; Sjostedt et al., 2017), respectively, were used as positive controls. As shown in Fig. 2A and B, ATP-dependent transport by MRP2 was observed for FMTX, ZV, LDG, CB, SR101 and pyranine, while LDV was not transported. Although uptake of the known substrate LY indicated functionality of ABCG2, transport of ZV, LDG, pyranine or SR101 by ABCG2 was not detected. On the other hand, we observed significant transport of LDV and a weak transport of CB by ABCG2. A weak ATP-dependent transport of SR101 was also present in control vesicles (Fig. 2B and D). To reveal the nature of the SR101 uptake observed in control vesicles, transport was measured using EDTA as a Mg^{2+} chelator or Na-orthovanadate as a general ATP-ase inhibitor. These experiments showed a Mg^{2+}-dependent and Na-orthovanadate sensitive transport of SR101, confirming the involvement of a yet undefined insect transporter in SR101 transport (Supplementary Figure S1).

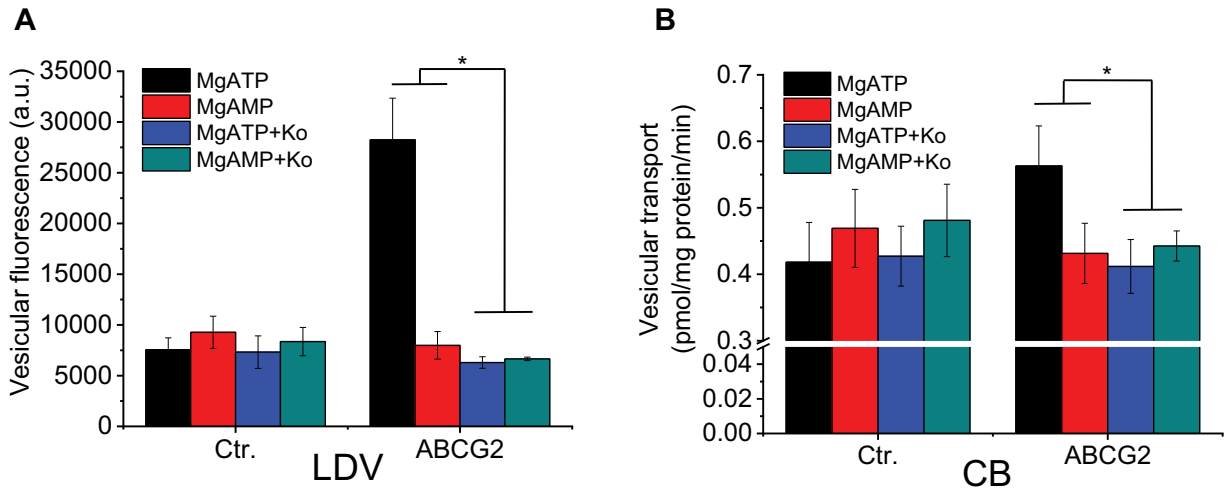

Fig. 6. Inhibition of LDV (panel A) or CB (panel B) uptake in IOVs containing ABCG2. Membrane vesicles (50 μg) were incubated in the presence or absence of 1 μM Ko143 for 5 minutes at 37°C. Transport reaction was started by the addition of 0.2 μl LDV/tube or 5 μM CB. Fluorescence after 10 minutes (LDV) or 30 minutes (CB) of incubation was determined using an Enspire plate reader. Experiments were repeated 3-times. Average +/- SD values are shown. Statistical significance was calculated between ATP-dependent signals. Delta values generated by subtracting MgAMP or MgAMP + Ko signal from the signal of MgATP or MgATP + Ko, respectively were compared for statistical significance by Student's t-test, *: $p < 0.05$.

3.3. Transcellular transport of pyranine, a novel common substrate of OATP1B1 and MRP2

In order to test whether the newly identified dual fluorescent substrates can indeed be applied for the simultaneous investigation of OATP1B1 and MRP2 function, we examined their transport in double transfected polarized MDCKII cells. Since the structure of ZV, LDG and LDV is unknown, these dyes were excluded from further experiments. First, stable MDCKII cell lines co-expressing these transporters, termed as MDCKII-MRP2-OATP1B1 or MDCKII-ABCG2-OATP1B1 were engineered (see 2.2.). Cell lines containing solely OATP1B1, MRP2, ABCG2 or mock transfected cells (MDCKII-1B1, MDCKII-MRP2, MDCKII-ABCG2 or MDCKII-Ctr.) served as controls. Expression was confirmed by Western blot analysis (Fig. 3A), and functionality of the transporters was verified by transport assays using known OATP1B1, MRP2 or ABCG2 substrates, CB, CaAM and DCV, respectively (Fig. 3B).

For transcellular transport measurements, MDCKII cells were grown on transwell inserts for 4 days to reach a polarized state, when OATP1B1 is localized to the basolateral membrane, and MRP2 or ABCG2 are found apically (Cui et al., 2001; Matsushima et al., 2005). First, FMTX, a previously identified substrate of OATP1B1 (Gui et al., 2010) and MRP2 (Notenboom et al., 2005; Prevoo et al., 2011) was used for the setup of the transcellular transport measurement. As shown on Fig. 3C, a time-dependent transcellular basolateral to apical (B-A) transport of FMTX could be observed in MRP2-OATP1B1 double transfectants that was not present in the control, single transfected MDCKII-1B1, MDCKII-MRP2 or MDCKII-Ctr. (mock) cells. Next, transcellular transport of pyranine was determined. As shown on Fig. 4A, a time-dependent B-A transport of pyranine could be observed in MRP2-OATP1B1 double transfectants, and there was no B-A transport in single or mock transfected cells. When intracellular accumulation of pyranine was measured, we found that pyranine cannot enter the cells without the function of OATP1B1, hence it cannot be detected in control or MRP2 single transfected cells (Fig. 4B). To exclude leakage of the cell monolayer, concurrent pyranine transport in the apical to basolateral (A–B) direction was investigated. Transport of pyranine in both directions was measured on the MRP2-OATP1B1 double and OATP1B1 single transfectant cells (Fig. 4C). We found negligible transcellular transport from the apical to the basal compartment in both cell lines. These results indicate that the B to A directed transport is indeed derived from the interaction of the dye with the OATP1B1 and MRP2 transporters. Finally, in order to verify that the increasing fluorescent pyranine signal at the A side of double transfected cells is a result of the concerted action of OATP1B1 and MRP2, the experiments were repeated in the presence of transporter inhibitors (Fig. 4D). Double transfected cells treated with either cyclosporin A at the basal side or benzbromarone at the apical side showed no detectable transcellular transport. To control these experiments, OATP1B1 and MRP2 single transfected cells were also treated with cyclosporin A or benzbromarone, at the basal or apical side, respectively. Taken together, the results were consistent with the transcellular transport of pyranine in double transfectants as a result of OATP1B1-mediated uptake and MRP2-mediated efflux.

3.4. Identification of Cascade Blue hydrazide and sulforhodamine 101 as dual OATP1B1 and MRP2 probes in transwell measurements

Based on the experiments evaluated in the *Sf9* IOV assay, SR101 is another potential common substrate of OATP1B1 and MRP2, and a weak accumulation of CB in IOVs with MRP2 or ABCG2 was also detected. Therefore, in order to test their applicability as fluorescent probes in vectorial transport measurements, their transcellular transport was investigated in transwell transport assays (Fig. 5). When following time dependent accumulation of CB or SR101 in the apical compartment of the transwells, vectorial transport in MRP2-OATP1B1 double transfected cells was detected for both substrates (Fig. 5A-B). Interestingly, although we detected ABCG2-mediated transport of CB in IOVs, transcellular transport activity in ABCG2-OATP1B1 cells could not be observed (Fig. 5A). Transcellular transport of CB and SR101 in the A-B direction was negligible (Fig. 5C), and inhibitory measurements performed with these dyes also confirmed OATP1B1- and MRP2-mediated transport of CB and SR101 (Fig. 5D).

4. Discussion

Concerted action of hepatic uptake (OATP) and efflux transporters (ABCC2 and ABCG2) is crucial in pharmacokinetics and in the disposition of therapeutic drugs and endogenous substances. Consequently, simultaneous administration of transporter substrates can lead to altered pharmacokinetics and undesired side effects. Therefore, international regulations require the evaluation of OATP1B1/3 and ABCG2 (and also potentially MRP2) during early

phases of drug development.

Polarized cell lines engineered to overexpress both uptake and efflux transporters are an accepted *in vitro* model of transepithelial transport measurements. MDCKII cells co-expressing OATP1B and MRP2 or OATP1B and ABCG2 have been used in numerous studies for the measurement of vectorial transport of common OATP and ABC transporter substrates (Cui et al., 2001; Fahrmayr et al., 2012; Matsushima et al., 2005). Double-transfected cell lines allow the identification of dual substrates (especially when the test compound cannot enter the cells without the contribution of an uptake transporter) and also the determination of the involvement of transporters in the transcellular transport (Matsushima, 2005; Sasaki, 2002). MDCKII cells co-expressing OATP and ABC transporters are also used to investigate DDIs mediated by these transporters (Cui et al., 2001; Fahrmayr et al., 2012; Liu et al., 2006; Matsushima et al., 2005).

Considering their overlapping substrate specificities, OATP1Bs, MRP2 and ABCG2 may also share common fluorescent substrates. Indeed, several mutual fluorescent probes were reported (e.g. FMTX Gui et al., 2010; Notenboom et al., 2005), cholyl-lysyl-fluorescein (Barber et al., 2015; de Waart et al., 2010) or carboxy-dichloro-fluorescein derivatives (Heredi-Szabo et al., 2008)). Although separate studies have identified common fluorescent substrates of MRP2 and OATP1Bs, these were not tested in double transfectants for vectorial transport. The only exception is Fluo-3 that has been used in transcellular transport experiments to investigate MRP2 and OATP1B3 function (Cui et al., 2001). However, Fluo-3 is not transported by the major hepatic OATP, OATP1B1 (Izumi et al., 2016), and application of fluorescent probes for dual investigation of ABCG2 and OATP1B function have not yet been documented. One crucial difference between an ideal probe substrate of uptake or efflux transporters is membrane permeability. Uptake transporters require substrates with low membrane permeability, while optimal efflux transporter substrates have high levels of passive uptake (at least in measurements performed on intact cells) (Bednarczyk, 2010; Gui et al., 2010; Kovacsics et al., 2017; Patik et al., 2018; Szakacs et al., 2008; Yamaguchi et al., 2006). However, shared substrates of uptake and efflux transporters can be identified using double transfected polarized cells, or in transport experiments using IOVs. IOVs allow the measurement of intravesicular accumulation of cell impermeable dyes by inversely oriented efflux transporters, and represent a faster and cheaper screening method compared to the transcellular transport assay. Hence, in our current work, the initial transport screens of the previously identified cell impermeable fluorescent OATP probes, and the novel dye substrate pyranine (Fig. 1B), were performed on IOVs containing MRP2 or ABCG2. First, in order to find an alternative for CB, we tested pyranine for transport by hepatic OATPs (Fig. 1B). We found that although pyranine is a lower affinity substrate compared to CB (pyranine Km values for OATP1B1, OATP1B3 and OATP2B1 were 27.8, 92.2 and 65.6 μM, respectively, vs. CB Km values were 2.6, 21 and 21 μM (Patik, 2018)), its transport by all three OATPs is about 3-times higher than that of CB. Therefore, we conclude that pyranine can be an excellent tool to investigate hepatic OATP function.

The IOV-based transport screen identified the hitherto undescribed transport of ZV, LDG, pyranine, SR101 and CB by MRP2, and LDV and CB transport by ABCG2 (Fig. 2). Interestingly, SR101 has been previously identified as a transported substrate of an MRP-like fish and rat transporter (Miller et al., 2002, 2000). However, direct interaction of this dye with human MRP2 has not yet been documented. After the IOV screen, the novel substrates were tested in OATP1B1-MRP2 double transfected MDCKII cells for basolateral to apical transport, which confirmed pyranine, CB and SR101 as dual probes of OATP1B1 and MRP2 (Figs. 4 and 5). In these experiments fluorescein-methotrexate, a previously identified substrate of both OATP1B1 and MRP2 served as positive control (Gui et al., 2010; Notenboom et al., 2005). Vectorial transport could be inhibited by known OATP MRP2 inhibitors, indicating that these fluorescent probes can be used for assessing drug interactions with OATP1B or MRP2.

Although CB transport was very low in MRP2 and ABCG2 containing IOVs, we still detected significant transport of this dye in double transfected MDCKII-MRP2-OATP1B1 cells. However, although expression and function of both OATP1B1 and ABCG2 was confirmed in the double transfected MDCKII cell line (Fig. 3A-B), we could not detect any transcellular transport of CB (Fig. 5A). These discrepancies can be explained by the conversion of CB in the cells (but not in IOVs) into a metabolite that is a higher affinity substrate of MRP2 than CB, but not recognized anymore by ABCG2. Mass spectrometry studies analyzing CB extruded from MDCKII-MRP2-OATP1B1 cells may clarify this issue. These results underline the relevance of cell-based assays, which are influenced by the intracellular metabolism of compounds that are also relevant in physiological drug transporter and drug-drug interactions.

Finally, since dual probes of OATP1B1 and ABCG2 suitable for transcellular transport measurements have not been identified, we also tested the transport of LDV, identified here as a substrate for ABCG2 (Fig. 2C). However, these experiments also failed to detect any vectorial transport in MDCKII-ABCG2-OATP1B1 cells (not shown). In addition, as LY has been described as a substrate of zebrafish drOatp1d1 (Faltermann et al., 2016), and our IOV experiments (Fig. 2D) showed high level of uptake of this compound by ABCG2, we tested LY transport in MDCKII-OATP1B1 cells. However, we found no detectable OATP1B1-mediated uptake of this compound (not shown), therefore LY was also excluded as a dual OATP1B1/ABCG2 probe. Although our efforts failed to set up an assay for vectorial transport of potential dual OATP1B1 and ABCG2 probes, LDV and CB can still be used to detect ABCG2 drug interactions in vesicular transport studies. As demonstrated in Fig. 6, uptake of these dyes in IOVs is inhibited in the presence of Ko143, a specific ABCG2 inhibitor (Fig. 6).

Although cell lines engineered to overexpress pairs of uptake and efflux transporter or even metabolic enzymes are an accepted model of *in vitro* drug interaction screens, to recapitulate *in vivo* conditions more complex models, e.g. human derived hepatocytes are needed. The dual OATP MRP2 substrates identified in our study are good candidates to monitor the function and drug interactions of these transporters in hepatocytes. Due to their low passive permeability, practically no uptake of pyranine, CB or SR101 is observed in mock transfected cells (Fig. 1B, and see also in Bakos et al., 2019; Patik et al., 2018), predicting low unspecific labeling in cellular assays/experiments. On the other hand, a plethora of transporters is present in hepatocytes, some of which may be involved in the uptake or efflux of these dyes. Based on our experiments, ABCG2 will not influence elimination of these dyes from the cells. In addition, based on our preliminary experiments performed with IOVs containing human ABCB1 (P-gp), no interaction with pyranine, CB or SR101 can be expected (not shown). However, it cannot be excluded that other ABC transporters, e.g. MRP3 (ABCC3), MRP4 (ABCC4), expressed in the sinusoidal membranes of hepatocytes, recognize these dyes and will limit their cellular accumulation. Similarly, the interaction of the fluorescent dyes with other solute carriers (SLCs) cannot be excluded. Future work will address the applicability of the fluorescence assays in more complex models. For example, toxicity of the test substrates may limit the applicability of these dyes in hepatocytes. However, when we investigated this issue in MDCKII cells we found no significant toxicity (Supplementary Fig. S2).

In conclusion we identify dual OATP1B1 MRP2 fluorescent probes, and also novel fluorescent substrates of ABCG2. To our best knowledge, pyranine, CB and SR101 are the first dual probes that can be applied for determining in a single, fluorescence-based assay the activity of OATP1B1 and MRP2 and for evaluating the DDI potential of drug candidates.

Authors' contribution

Virág Székely: performed the experiments, analyzed the data, helped in original draft preparation **Izabel Patik**: performed the

experiments, contributed to the design of the expriments, **Orsolya Ungvári**: performed the experiments, analyzed data**Ágnes Telbisz:** performed the experiments, helped in reviewing and editing the manuscript**Gergely Szakács**: helped in reviewing and editing the manuscript, **Éva Bakos**: Supervision, writing, original draft preparation **Csilla Özvegy-Laczka:**conceptualization, writing.

Declaration of Competing Interest

None.

Acknowledgements

This work has been supported by a research grant from the National Research, Development and Innovation Office [OTKA FK 128751]. Cs. Ö-L. is a recipient of the János Bolyai fellowship of the Hungarian Academy of Sciences.

Supplementary materials

Supplementary material associated with this article can be found, in the online version, at doi:10.1016/j.ejps.2020.105395.

References

Allen, J.D., van Loevezijn, A., Lakhai, J.M., van der Valk, M., van Tellingen, O., Reid, G., Schellens, J.H., Koomen, G.J., Schinkel, A.H., 2002. Potent and specific inhibition of the breast cancer resistance protein multidrug transporter in vitro and in mouse intestine by a novel analogue of fumitremorgin C. Mol. Cancer Ther. 1, 417–425.

Avnir, Y., Barenholz, Y., 2005. pH determination by pyranine: medium-related artifacts and their correction. Anal. Biochem. 347, 34–41.

Badee, J., Achour, B., Rostami-Hodjegan, A., Galetin, A., 2015. Meta-analysis of expression of hepatic organic anion-transporting polypeptide (OATP) transporters in cellular systems relative to human liver tissue. Drug Metab. Disposition Biol. Fate Chem. 43, 424–432.

Bakos, E., Evers, R., Sinko, E., Varadi, A., Borst, P., Sarkadi, B., 2000. Interactions of the human multidrug resistance proteins MRP1 and MRP2 with organic anions. Mol. Pharmacol. 57, 760–768.

Bakos, E., Nemet, O., Patik, I., Kucsma, N., Varady, G., Szakacs, G., Ozvegy-Laczka, C., 2019. A novel fluorescence-based functional assay for human OATP1A2 and OATP1C1 identifies interaction between third generation P-gp inhibitors and OATP1A2. FEBS J.

Barber, J.A., Stahl, S.H., Summers, C., Barrett, G., Park, B.K., Foster, J.R., Kenna, J.G., 2015. Quantification of drug-induced inhibition of canalicular Cholyl-l-Lysyl-fluorescein excretion from hepatocytes by high content cell imaging. Toxicol. Sci. 148, 48–59.

Bednarczyk, D., 2010. Fluorescence-based assays for the assessment of drug interaction with the human transporters OATP1B1 and OATP1B3. Anal. Biochem. 405, 50–58.

Cantz, T., Nies, A.T., Brom, M., Hofmann, A.F., Keppler, D., 2000. MRP2, a human conjugate export pump, is present and transports fluo 3 into apical vacuoles of Hep G2 cells. Am. J. Physiol. Gastrointest. Liver Physiol. 278, G522–G531.

Clement, N.R., Gould, J.M., 1981. Pyranine (8-hydroxy-1,3,6-pyrenetrisulfonate) as a probe of internal aqueous hydrogen ion concentration in phospholipid vesicles. Biochemistry 20, 1534–1538.

Cui, Y., Konig, J., Keppler, D., 2001. Vectorial transport by double-transfected cells expressing the human uptake transporter SLC21A8 and the apical export pump ABCC2. Mol. Pharmacol. 60, 934–943.

Dawson, P.A., Lan, T., Rao, A., 2009. Bile acid transporters. J. Lipid Res. 50, 2340–2357.

de Waart, D.R., Hausler, S., Vlaming, M.L., Kunne, C., Hanggi, E., Gruss, H.J., Oude Elferink, R.P., Stieger, B., 2010. Hepatic transport mechanisms of cholyl-L-lysyl-fluorescein. J. Pharmacol. Exp. Ther. 334, 78–86.

Deng, F., Sjostedt, N., Kidron, H., 2016. The effect of albumin on MRP2 and BCRP in the vesicular transport assay. PLoS One 11, e0163886.

Doyle, L.A., Yang, W., Abruzzo, L.V., Krogmann, T., Gao, Y., Rishi, A.K., Ross, D.D., 1998. A multidrug resistance transporter from human MCF-7 breast cancer cells. PNAS 95, 15665–15670.

Fahrmayr, C., Konig, J., Auge, D., Mieth, M., Fromm, M.F., 2012. Identification of drugs and drug metabolites as substrates of multidrug resistance protein 2 (MRP2) using triple-transfected MDCK-OATP1B1-UGT1A1-MRP2 cells. Br. J. Pharmacol. 165, 1836–1847.

Faltermann, S., Pretot, R., Pernthaler, J., Fent, K., 2016. Comparative effects of nodularin and microcystin-LR in zebrafish: 1. Uptake by organic anion transporting polypeptide Oatp1d1 (Slco1d1). Aquat. Toxicol. 171, 69–76.

Gan, B.S., Krump, E., Shrode, L.D., Grinstein, S., 1998. Loading pyranine via purinergic receptors or hypotonic stress for measurement of cytosolic pH by imaging. Am. J. Physiol. 275, C1158–C1166.

Giacomini, K.M., Balimane, P.V., Cho, S.K., Eadon, M., Edeki, T., Hillgren, K.M., Huang, S.M., Sugiyama, Y., Weitz, D., Wen, Y., Xia, C.Q., Yee, S.W., Zimdahl, H., Niemi, M., International Transporter, C., 2013. International transporter consortium commentary on clinically important transporter polymorphisms. Clin. Pharmacol. Ther. 94, 23–26.

Giacomini, K.M., Huang, S.M., 2013. Transporters in drug development and clinical pharmacology. Clin. Pharmacol. Ther. 94, 3–9.

Giacomini, K.M., Huang, S.M., Tweedie, D.J., Benet, L.Z., Brouwer, K.L., Chu, X., Dahlin, A., Evers, R., Fischer, V., Hillgren, K.M., Hoffmaster, K.A., Ishikawa, T., Keppler, D., Kim, R.B., Lee, C.A., Niemi, M., Polli, J.W., Sugiyama, Y., Swaan, P.W., Ware, J.A., Wright, S.H., Yee, S.W., Zamek-Gliszczynski, M.J., Zhang, L., 2010. Membrane transporters in drug development. Nat. Rev. Drug Discov. 9, 215–236.

Gui, C., Obaidat, A., Chaguturu, R., Hagenbuch, B., 2010. Development of a cell-based high-throughput assay to screen for inhibitors of organic anion transporting polypeptides 1B1 and 1B3. Curr. Chem. Genomics 4, 1–8.

Hagenbuch, B., Stieger, B., 2013. The SLCO (former SLC21) superfamily of transporters. Mol. Aspects Med. 34, 396–412.

Heredi-Szabo, K., Kis, E., Molnar, E., Gyorfi, A., Krajcsi, P., 2008. Characterization of 5(6)-carboxy-2,'7'-dichlorofluorescein transport by MRP2 and utilization of this substrate as a fluorescent surrogate for LTC4. J. Biomol. Screen 13, 295–301.

Heyes, N., Kapoor, P., Kerr, I.D., 2018. Polymorphisms of the multidrug Pump ABCG2: a systematic review of their effect on protein expression, function, and drug pharmacokinetics. Drug Metab. Disposition Biol. Fate Chem. 46, 1886–1899.

Hirano, M., Maeda, K., Matsushima, S., Nozaki, Y., Kusuhara, H., Sugiyama, Y., 2005. Involvement of BCRP (ABCG2) in the biliary excretion of pitavastatin. Mol. Pharmacol. 68, 800–807.

Hirouchi, M., Kusuhara, H., Onuki, R., Ogilvie, B.W., Parkinson, A., Sugiyama, Y., 2009. Construction of triple-transfected cells [organic anion-transporting polypeptide (OATP) 1B1/multidrug resistance-associated protein (MRP) 2/MRP3 and OATP1B1/MRP2/MRP4] for analysis of the sinusoidal function of MRP3 and MRP4. Drug Metab. Disposition Biol. Fate Chem. 37, 2103–2111.

Hollo, Z., Homolya, L., Davis, C.W., Sarkadi, B., 1994. Calcein accumulation as a fluorometric functional assay of the multidrug transporter. Biochim. Biophys. Acta 1191, 384–388.

Hooijberg, J.H., Broxterman, H.J., Kool, M., Assaraf, Y.G., Peters, G.J., Noordhuis, P., Scheper, R.J., Borst, P., Pinedo, H.M., Jansen, G., 1999. Antifolate resistance mediated by the multidrug resistance proteins MRP1 and MRP2. Cancer Res. 59, 2532–2535.

Horsey, A.J., Cox, M.H., Sarwat, S., Kerr, I.D., 2016. The multidrug transporter ABCG2: still more questions than answers. Biochem. Soc. Trans. 44, 824–830.

Izumi, S., Nozaki, Y., Komori, T., Takenaka, O., Maeda, K., Kusuhara, H., Sugiyama, Y., 2016. Investigation of fluorescein derivatives as substrates of organic anion transporting polypeptide (OATP) 1B1 to develop sensitive fluorescence-based OATP1B1 inhibition assays. Mol. Pharm. 13, 438–448.

Jedlitschky, G., Hoffmann, U., Kroemer, H.K., 2006. Structure and function of the MRP2 (ABCC2) protein and its role in drug disposition. Expert Opin. Drug Metab. Toxicol. 2, 351–366.

Jetter, A., Kullak-Ublick, G.A., 2019. Drugs and hepatic transporters: a review. Pharmacol. Res., 104234.

Kimoto, E., Yoshida, K., Balogh, L.M., Bi, Y.A., Maeda, K., El-Kattan, A., Sugiyama, Y., Lai, Y., 2012. Characterization of organic anion transporting polypeptide (OATP) expression and its functional contribution to the uptake of substrates in human hepatocytes. Mol. Pharm. 9, 3535–3542.

Kitamura, S., Maeda, K., Wang, Y., Sugiyama, Y., 2008. Involvement of multiple transporters in the hepatobiliary transport of rosuvastatin. Drug Metab. Disposition Biol. Fate Chem. 36, 2014–2023.

Kock, K., Brouwer, K.L., 2012. A perspective on efflux transport proteins in the liver. Clin. Pharmacol. Ther. 92, 599–612.

Konig, J., Cui, Y., Nies, A.T., Keppler, D., 2000. A novel human organic anion transporting polypeptide localized to the basolateral hepatocyte membrane. Am. J. Physiol. Gastrointest. Liver Physiol. 278, G156–G164.

Konig, J., Nies, A.T., Cui, Y., Leier, I., Keppler, D., 1999. Conjugate export pumps of the multidrug resistance protein (MRP) family: localization, substrate specificity, and MRP2-mediated drug resistance. Biochim. Biophys. Acta 1461, 377–394.

Kovacsics, D., Patik, I., Ozvegy-Laczka, C., 2017. The role of organic anion transporting polypeptides in drug absorption, distribution, excretion and drug-drug interactions. Expert Opin. Drug Metab. Toxicol. 13, 409–424.

Kullak-Ublick, G.A., Ismair, M.G., Stieger, B., Landmann, L., Huber, R., Pizzagalli, F., Fattinger, K., Meier, P.J., Hagenbuch, B., 2001. Organic anion-transporting polypeptide B (OATP-B) and its functional comparison with three other OATPs of human liver. Gastroenterology 120, 525–533.

Lee, C.A., O'Connor, M.A., Ritchie, T.K., Galetin, A., Cook, J.A., Ragueneau-Majlessi, I., Ellens, H., Feng, B., Taub, M.E., Paine, M.F., Polli, J.W., Ware, J.A., Zamek-Gliszczynski, M.J., 2015. Breast cancer resistance protein (ABCG2) in clinical pharmacokinetics and drug interactions: practical recommendations for clinical victim and perpetrator drug-drug interaction study design. Drug Metab. Disposition Biol. Fate Chem. 43, 490–509.

Link, E., Parish, S., Armitage, J., Bowman, L., Heath, S., Matsuda, F., Gut, I., Lathrop, M., Collins, R., 2008. SLCO1B1 variants and statin-induced myopathy–a genomewide study. N. Engl. J. Med. 359, 789–799.

Liu, L., Cui, Y., Chung, A.Y., Shitara, Y., Sugiyama, Y., Keppler, D., Pang, K.S., 2006. Vectorial transport of enalapril by Oatp1a1/Mrp2 and OATP1B1 and OATP1B3/MRP2 in rat and human livers. J. Pharmacol. Exp. Ther. 318, 395–402.

Liu, Y.H., Di, Y.M., Zhou, Z.W., Mo, S.L., Zhou, S.F., 2010. Multidrug resistance-associated proteins and implications in drug development. Clin. Exp. Pharmacol. Physiol. 37, 115–120.

Maliepaard, M., Scheffer, G.L., Faneyte, I.F., van Gastelen, M.A., Pijnenborg, A.C., Schinkel, A.H., van De Vijver, M.J., Scheper, R.J., Schellens, J.H., 2001. Subcellular

localization and distribution of the breast cancer resistance protein transporter in normal human tissues. Cancer Res. 61, 3458–3464.
Mao, Q., Unadkat, J.D., 2015. Role of the breast cancer resistance protein (BCRP/ABCG2) in drug transport–an update. AAPS J. 17, 65–82.
Mathew, G., Timm Jr., E.A., Sotomayor, P., Godoy, A., Montecinos, V.P., Smith, G.J., Huss, W.J., 2009. ABCG2-mediated DyeCycle Violet efflux defined side population in benign and malignant prostate. Cell Cycle 8, 1053–1061.
Matsuo, H., Takada, T., Ichida, K., Nakamura, T., Nakayama, A., Ikebuchi, Y., Ito, K., Kusanagi, Y., Chiba, T., Tadokoro, S., Takada, Y., Oikawa, Y., Inoue, H., Suzuki, K., Okada, R., Nishiyama, J., Domoto, H., Watanabe, S., Fujita, M., Morimoto, Y., Naito, M., Nishio, K., Hishida, A., Wakai, K., Asai, Y., Niwa, K., Kamakura, K., Nonoyama, S., Sakurai, Y., Hosoya, T., Kanai, Y., Suzuki, H., Hamajima, N., Shinomiya, N., 2009. Common defects of ABCG2, a high-capacity urate exporter, cause gout: a function-based genetic analysis in a Japanese population. Sci. Transl. Med. 1, 5ra11.
Matsushima, S., Maeda, K., Kondo, C., Hirano, M., Sasaki, M., Suzuki, H., Sugiyama, Y., 2005. Identification of the hepatic efflux transporters of organic anions using double-transfected Madin-Darby canine kidney II cells expressing human organic anion-transporting polypeptide 1B1 (OATP1B1)/multidrug resistance-associated protein 2, OATP1B1/multidrug resistance 1, and OATP1B1/breast cancer resistance protein. J. Pharmacol. Exp. Ther. 314, 1059–1067.
Miller, D.S., Graeff, C., Droulle, L., Fricker, S., Fricker, G., 2002. Xenobiotic efflux pumps in isolated fish brain capillaries. Am. J. Physiol. Regul. Integr. Comp. Physiol. 282, R191–R198.
Miller, D.S., Nobmann, S.N., Gutmann, H., Toeroek, M., Drewe, J., Fricker, G., 2000. Xenobiotic transport across isolated brain microvessels studied by confocal microscopy. Mol. Pharmacol. 58, 1357–1367.
Notenboom, S., Miller, D.S., Kuik, L.H., Smits, P., Russel, F.G., Masereeuw, R., 2005. Short-term exposure of renal proximal tubules to gentamicin increases long-term multidrug resistance protein 2 (Abcc2) transport function and reduces nephrotoxicant sensitivity. J. Pharmacol. Exp. Ther. 315, 912–920.
Ozvegy, C., Varadi, A., Sarkadi, B., 2002. Characterization of drug transport, ATP hydrolysis, and nucleotide trapping by the human ABCG2 multidrug transporter. Modulation of substrate specificity by a point mutation. J. Biol. Chem. 277, 47980–47990.
Patel, M., Taskar, K.S., Zamek-Gliszczynski, M.J., 2016. Importance of hepatic transporters in clinical disposition of drugs and their metabolites. J. Clin. Pharmacol. 56 (Suppl 7), S23–S39.
Patik, I., Kovacsics, D., Nemet, O., Gera, M., Varady, G., Stieger, B., Hagenbuch, B., Szakacs, G., Ozvegy-Laczka, C., 2015. Functional expression of the 11 human Organic Anion Transporting Polypeptides in insect cells reveals that sodium fluorescein is a general OATP substrate. Biochem. Pharmacol. 98, 649–658.
Patik, I., Szekely, V., Nemet, O., Szepesi, A., Kucsma, N., Varady, G., Szakacs, G., Bakos, E., Ozvegy-Laczka, C., 2018. Identification of novel cell-impermeant fluorescent substrates for testing the function and drug interaction of Organic Anion-Transporting Polypeptides, OATP1B1/1B3 and 2B1. Sci. Rep. 8, 2630.
Prasad, B., Evers, R., Gupta, A., Hop, C.E., Salphati, L., Shukla, S., Ambudkar, S.V., Unadkat, J.D., 2014. Interindividual variability in hepatic organic anion-transporting polypeptides and P-glycoprotein (ABCB1) protein expression: quantification by liquid chromatography tandem mass spectroscopy and influence of genotype, age, and sex. Drug Metab. Disposition Biol. Fate Chem. 42, 78–88.
Prevoo, B., Miller, D.S., van de Water, F.M., Wever, K.E., Russel, F.G., Flik, G., Masereeuw, R., 2011. Rapid, nongenomic stimulation of multidrug resistance protein 2 (Mrp2) activity by glucocorticoids in renal proximal tubule. J. Pharmacol. Exp. Ther. 338, 362–371.
Roth, M., Obaidat, A., Hagenbuch, B., 2012. OATPs, OATs and OCTs: the organic anion and cation transporters of the SLCO and SLC22A gene superfamilies. Br. J. Pharmacol. 165, 1260–1287.
Saranko, H., Tordai, H., Telbisz, A., Ozvegy-Laczka, C., Erdos, G., Sarkadi, B., Hegedus, T., 2013. Effects of the gout-causing Q141K polymorphism and a CFTR DeltaF508 mimicking mutation on the processing and stability of the ABCG2 protein. Biochem. Biophys. Res. Commun. 437, 140–145.
Sarkadi, B., Price, E.M., Boucher, R.C., Germann, U.A., Scarborough, G.A., 1992. Expression of the human multidrug resistance cDNA in insect cells generates a high activity drug-stimulated membrane ATPase. J. Biol. Chem. 267, 4854–4858.
Shitara, Y., 2011. Clinical importance of OATP1B1 and OATP1B3 in drug-drug interactions. Drug Metab. Pharmacokinet. 26, 220–227.
Shitara, Y., Itoh, T., Sato, H., Li, A.P., Sugiyama, Y., 2003. Inhibition of transporter-mediated hepatic uptake as a mechanism for drug-drug interaction between cerivastatin and cyclosporin A. J. Pharmacol. Exp. Ther. 304, 610–616.
Siissalo, S., Hannukainen, J., Kolehmainen, J., Hirvonen, J., Kaukonen, A.M., 2009. A Caco-2 cell based screening method for compounds interacting with MRP2 efflux protein. Eur. J. Pharm. Biopharm. 71, 332–338.
Sjostedt, N., van den Heuvel, J., Koenderink, J.B., Kidron, H., 2017. Transmembrane domain single-nucleotide polymorphisms impair expression and transport activity of ABC transporter ABCG2. Pharm. Res. 34, 1626–1636.
Szakacs, G., Varadi, A., Ozvegy-Laczka, C., Sarkadi, B., 2008. The role of ABC transporters in drug absorption, distribution, metabolism, excretion and toxicity (ADME-Tox). Drug Discov. Today 13, 379–393.
Telbisz, A., Muller, M., Ozvegy-Laczka, C., Homolya, L., Szente, L., Varadi, A., Sarkadi, B., 2007. Membrane cholesterol selectively modulates the activity of the human ABCG2 multidrug transporter. Biochim. Biophys. Acta 1768, 2698–2713.
van de Steeg, E., Stranecky, V., Hartmannova, H., Noskova, L., Hrebicek, M., Wagenaar, E., van Esch, A., de Waart, D.R., Oude Elferink, R.P., Kenworthy, K.E., Sticova, E., al-Edreesi, M., Knisely, A.S., Kmoch, S., Jirsa, M., Schinkel, A.H., 2012. Complete OATP1B1 and OATP1B3 deficiency causes human Rotor syndrome by interrupting conjugated bilirubin reuptake into the liver. J. Clin. Invest. 122, 519–528.
Woodward, O.M., Kottgen, A., Coresh, J., Boerwinkle, E., Guggino, W.B., Kottgen, M., 2009. Identification of a urate transporter, ABCG2, with a common functional polymorphism causing gout. PNAS 106, 10338–10342.
Yamaguchi, H., Okada, M., Akitaya, S., Ohara, H., Mikkaichi, T., Ishikawa, H., Sato, M., Matsuura, M., Saga, T., Unno, M., Abe, T., Mano, N., Hishinuma, T., Goto, J., 2006. Transport of fluorescent chenodeoxycholic acid via the human organic anion transporters OATP1B1 and OATP1B3. J. Lipid Res. 47, 1196–1202.
Zhou, S.F., Wang, L.L., Di, Y.M., Xue, C.C., Duan, W., Li, C.G., Li, Y., 2008. Substrates and inhibitors of human multidrug resistance associated proteins and the implications in drug development. Curr. Med. Chem. 15, 1981–2039.